

SUPPLEMENTARY MATERIALS AND METHODS

Cell cultures

The hTERT-immortalized human fibroblasts GM01604 (normal) and AG12975 (Werner syndrome) were obtained from Coriell Cell Repositories (Camden, NJ, USA). The hTERT fibroblasts were cultured in DMEM (Life Technologies, Carlsbad, CA, USA) with 15% FBS (Boehringer, Mannheim, Germany). Cells were incubated at 37 °C in a 5% CO₂ atmosphere.

Chemicals and treatment

Nocodazole (Sigma-Aldrich) was used at final concentration of 0.5 µg/ml to accumulate cells in M-phase.

Cell cycle analysis by flow cytometry

Cells were treated with Aph 0.4 µM and harvested at the indicated times. Cells were processed for flow cytometry as described (1) and data analysed with CellQuest software.

Evaluation of mitotic index by phospho-H3 immunostaining

For evaluation of mitotic index, 3×10^5 cells were plated in 35-mm dishes and exposed to 0.4 µM Aph for 16, 24 h before fixation in 2% PFA. After permeabilization in 0.5% Triton X-100, cells were blocked in 10% FBS and incubated with anti-pH3 antibody (Santa Cruz Biotechnology, Inc.) for 1 h at RT, followed by three washes in PBS and incubation with an Alexa 488-conjugated secondary antibody before DAPI counterstaining and evaluation of mitotic index by fluorescence microscopy.

Immunofluorescence

Immunofluorescence was performed as previously described (1). Staining with anti-RPA32 (Cambiochem) was performed as previously described (2). Slides were analyzed with a microscope (Leica) equipped with a charge-coupled device camera (Photometrics). Images were acquired as greyscale files using Metaview software (MDS Analytical Technologies) and processed using Adobe Photoshop CS3 (Adobe). For each time point, at least 100 nuclei were examined by two independent investigators and foci were scored at 60×. Only nuclei showing more than five bright foci were counted as positive. Parallel samples either incubated with the appropriate normal serum or only with the secondary antibody confirmed that the observed fluorescence pattern was not attributable to artifacts.

To detect parental-strand ssDNA, cells were prelabeled for 24 h with 10 μ M BrdU (Sigma-Aldrich), then 0.4 μ M Aph was added for 8 h. Next, cells were washed with PBS, permeabilized with 0.5% Triton X-100 for 10 min at 4°C and fixed as previously described (Couch et al., 2013). Fixed cells were then incubated with mouse anti-BrdU antibody (BD Pharmingen) for 1 h at RT 1% BSA/PBS, followed by specie-specific fluorescein-conjugated secondary antibodies (Jackson ImmunoResearch Laboratories), and counterstained with 0.5 μ g/ml DAPI. Images were acquired as reported above.

FISH

A mix of bacterial artificial chromosomes (BACs): BAC36B6 (RP-11) or BAC264L1 (RP-11), mapping, respectively, to FRA7H or FRA16D fragile site regions, were used as probes for FISH analyses.

SUPPLEMENTARY LEGENDS TO FIGURES

Figure S1. Analysis of CHK1 following robust genome-wide replication arrest. Western blot detection of CHK1 phosphorylation in WS cells (WS) and cells in which wild-type WRN was reintroduced (WSWRN) treated with 4 μ M Aph or 1 mM HU for the indicated time points. The presence of phosphorylated CHK1 was assessed using phospho-specific antibodies (pS345). Lamin B1 was used as loading control.

Figure S2. Analysis of CHK1 activation after mild replication perturbation. Western blot detection of CHK1 phosphorylation in total extracts of hTERT-immortalized primary fibroblasts, both WRN-proficient (GM01604) and WRN-deficient (AG12975), untreated (-) or treated with 0.4 μ M Aph at the indicated times. The presence of phosphorylated CHK1 was assessed using phospho-specific antibodies (pS345). Total amount of CHK1 was determined with an anti-CHK1 antibody. Lamin B1 was used as loading control.

Figure S3. Analysis of cell cycle progression upon moderate replication stress. **(A)** Wild-type (WSWRN) and WS cells were treated with 0.4 μ M Aph at various periods of time as indicated, then harvested and stained with PI prior to FACS analysis. Upper panel represents DNA content profiles of cells. Graph shows the percentage of cells distributed into G0/G1, S or G2/M phases. **(B)** Evaluation of mitotic cells in WSWRN and WS cells treated with 0.4 μ M Aph for the indicated times, estimated following 16 or 24 h in the presence of 0.5 μ g/ml nocodazole for 6 h before harvesting.. Mitotic index was determined as the number of histone H3-pSer10 positive cells over

the total cell population by immunofluorescence. Values are reported as mean from three independent experiments. Error bars represent standard error.

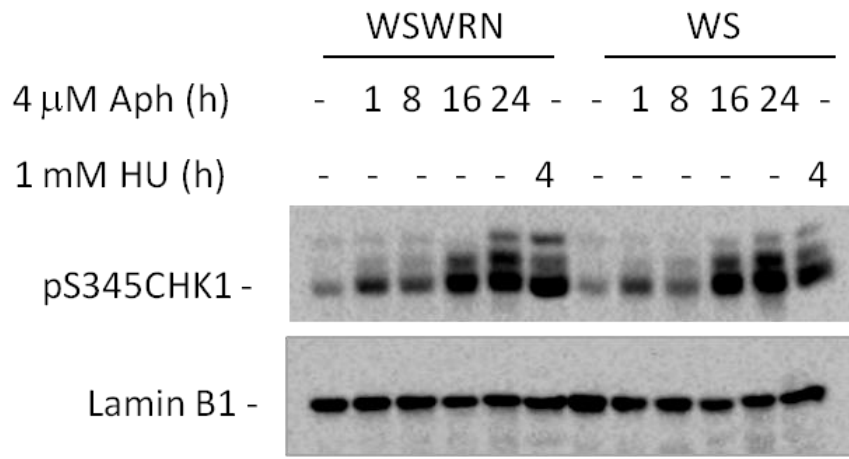
Figure S4. Cell cycle progression analysis following mild replication stress. **(A)** Graph shows the percentage of cells distributed into G0/G1, S or G2/M phases. WS cells and WS cells complemented with wild-type (WSWRN) or mutant form of WRN affecting helicase activity (WRN-K577M) were treated or not with Aph 0.4 μ M for the indicated times. Cells were harvested and stained with PI prior to FACS analysis. **(B)** The panel represents DNA content profiles of WRN-K577M cells.

Figure S5. Analysis of RPA32 accumulation and ssDNA formation in cells upon mild replication perturbation. **(A)** Immunostaining of cells with RPA32. Wild-type (WSWRN) and WS cells were untreated or treated with 0.4 μ M Aph at various periods of time as indicated and then processed for immunofluorescence analysis with a specific anti-RPA32 antibody. The Graph shows the percentages of RPA32-positive cells. Images of cells stained for RPA32 after 8 h exposure with Aph are reported. Nuclei were counterstained with DAPI. **(B)** Detection of BrdU incorporation under non-denaturing conditions in the parental DNA of wild-type (WSWRN) and WS cells treated as indicated (see “Materials and Methods” for details). Cells were stained with antibodies to BrdU and counterstained with DAPI. Graph shows the percentages of ssDNA formation evaluated as number of BrdU-positive nuclei. Values are reported as mean from three independent experiments. Error bars represent standard error. **(C)** Dot plot of the number of ssDNA foci per cell for a representative experiment in cells treated as in (A) is shown. Horizontal lines represent the medians of ssDNA foci formation.

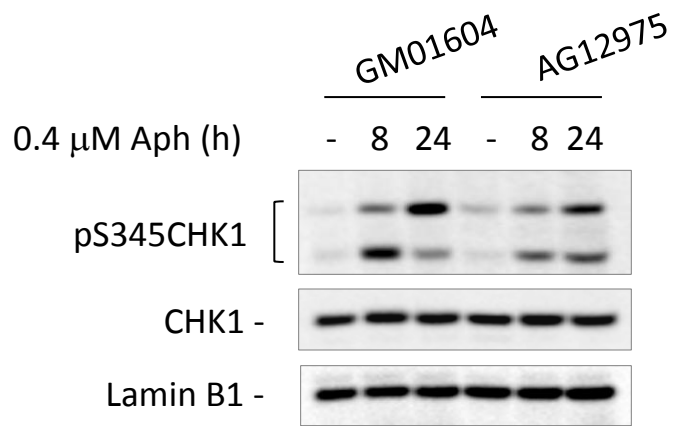
Figure S6. Analysis of CFS expression in cells expressing an ATR-unphosphorylatable form of WRN. Frequency of fragile site FRA7H and FRA16D expression in WS cells (WS), WS cells expressing an ATR-unphosphorylatable form of WRN (WSWRN^{6A}) and in WS cells in which wild-type WRN was reintroduced (WSWRN). Cells were treated the indicated doses of Aph and harvested 24 h later. Frequency of fragile site induction is presented as the percentage of chromosome 7 or 16 homologues with gaps and breaks at FRA7H and FRA16D, respectively. Data are presented as means of three independent experiments. Error bars represent standard error.

REFERENCES

1. Franchitto, A., Pirzio, L.M., Prosperi, E., Sapora, O., Bignami, M. and Pichierri, P. (2008) Replication fork stalling in WRN-deficient cells is overcome by prompt activation of a MUS81-dependent pathway. *J Cell Biol*, **183**, 241-252.
2. Ammazalorso, F., Pirzio, L.M., Bignami, M., Franchitto, A. and Pichierri, P. (2010) ATR and ATM differently regulate WRN to prevent DSBs at stalled replication forks and promote replication fork recovery. *EMBO J*, **29**, 3156-3169.

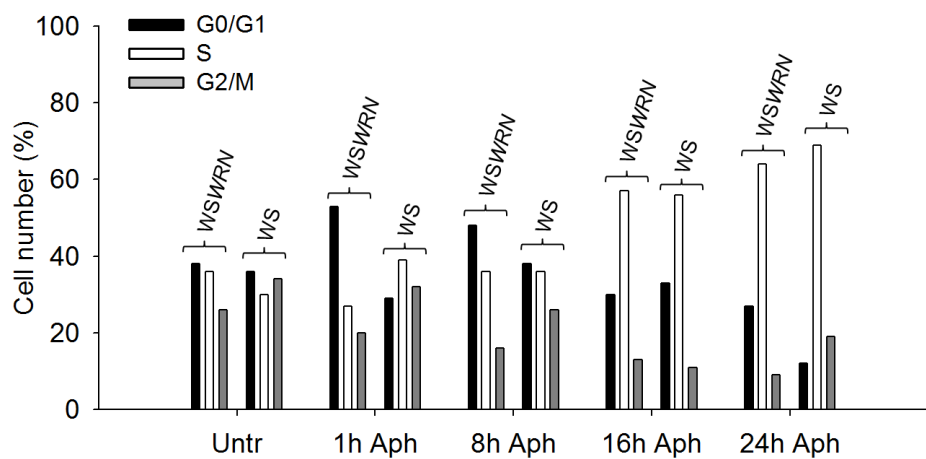
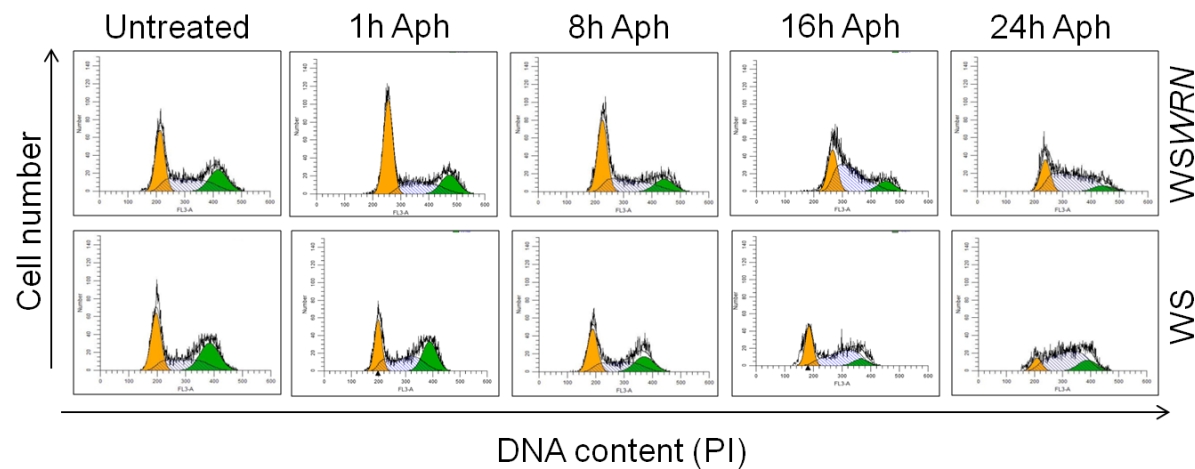


Supplementary Figure S1

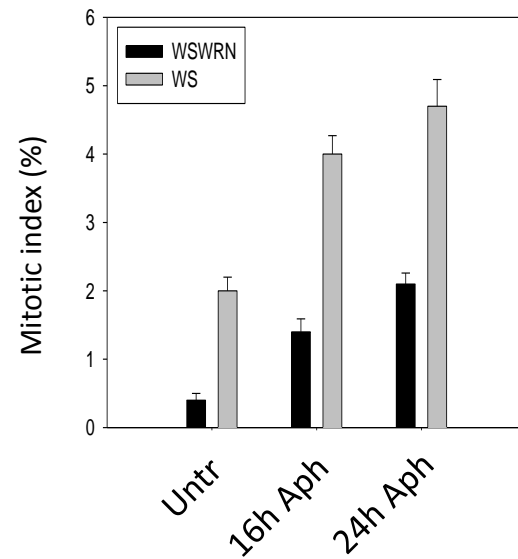


Supplementary Figure S2

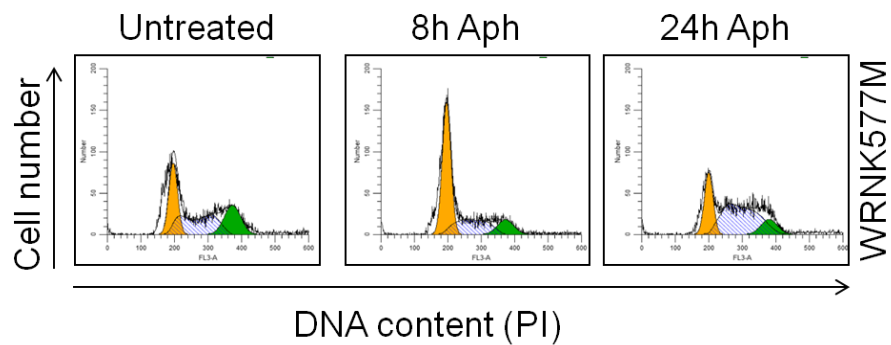
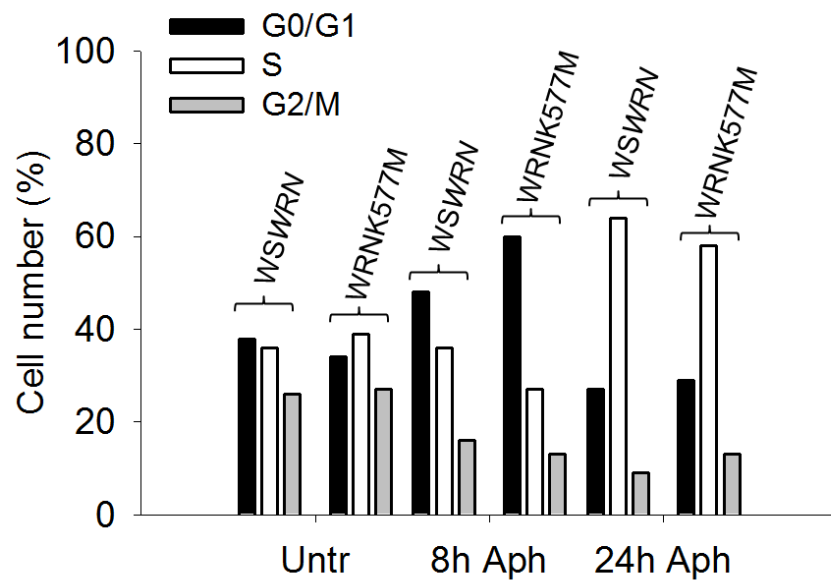
A



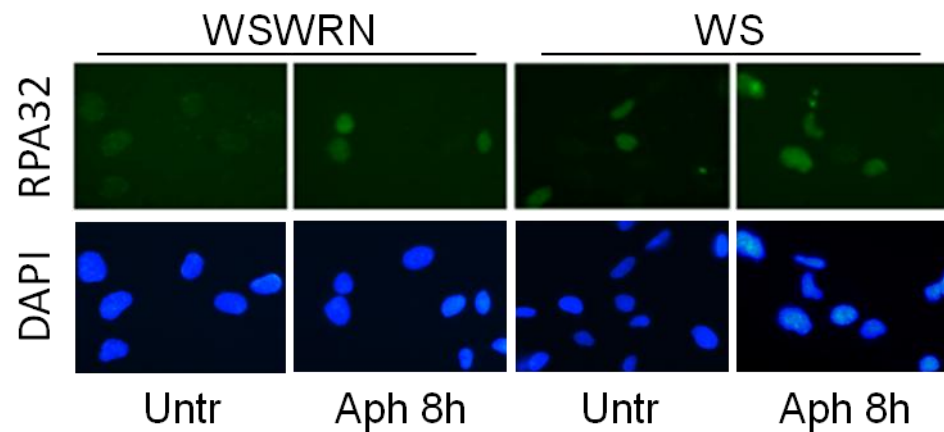
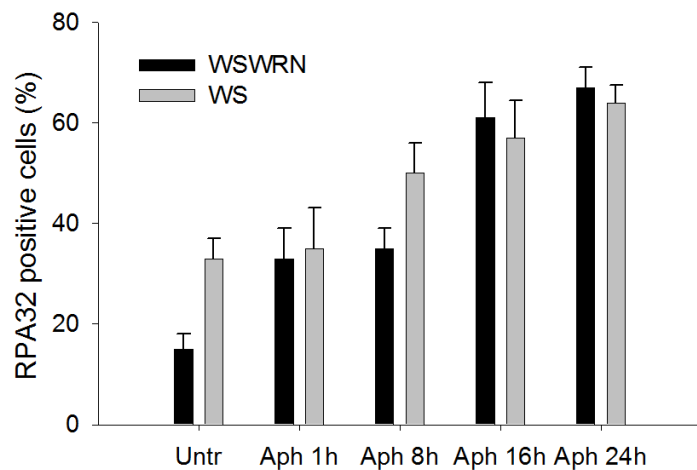
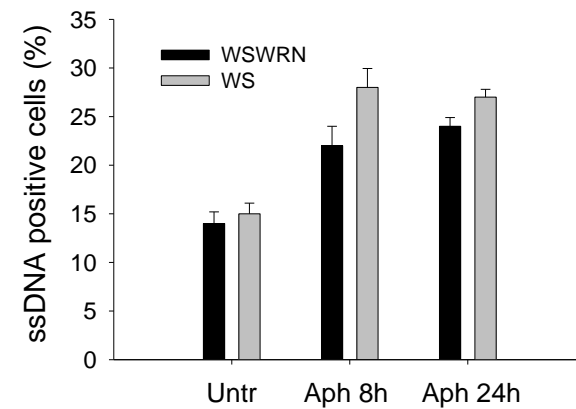
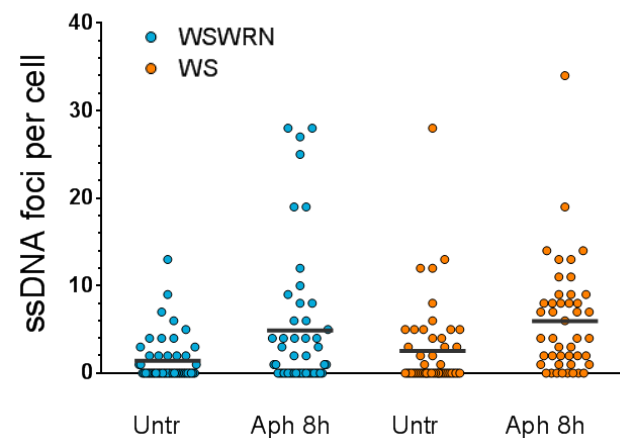
B

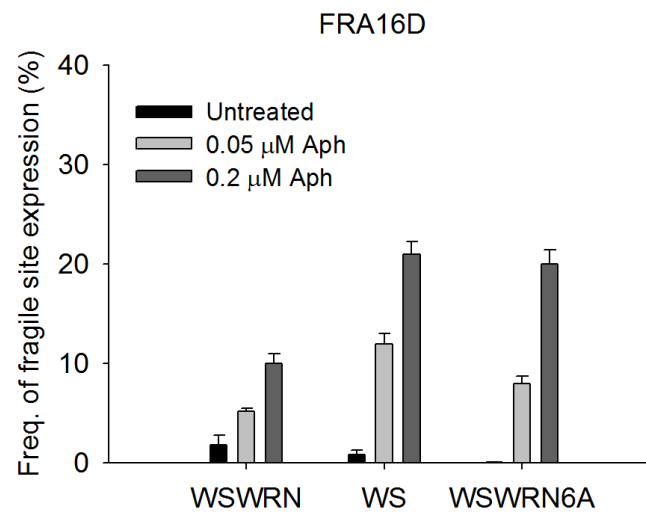
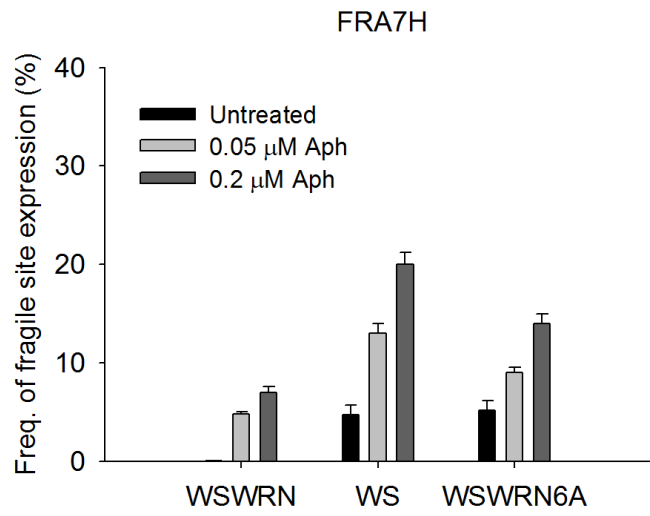


Supplementary Figure S3



Supplementary Figure S4

A**B****C**



Supplementary Figure S6